Real-time compensation of static distortion by measurement of differential noise gain

Lachlan J. Gunn, Andrew Allison, Derek Abbott
School of Electrical and Electronic Engineering
The University of Adelaide, SA 5005, Australia
lachlan.gunn@adelaide.edu.au

***Abstract*—It is well-known that in a cascaded system of amplifiers the majority of noise is due to the first stage and the majority of distortion due to the final stage. Consequently, the observed noise at the output is subject to the same nonlinear process as the signal of interest. We use this fact to characterise the distorting process and linearise the system in real-time using statistical measurements of this noise.**

I. Introduction

Many practical systems suffer from a measurable degree of nonlinearity despite the best efforts of their designers. In amplifiers this can be countered using negative feedback, however this comes at the cost of gain and so may require the use of additional gain stages and therefore cost. However, the use of feedback is not possible with all nonlinear components—consider, for example, a sensor measuring some physical quantity—and in these cases linear operation must be achieved by other means.

Filtering provides a partial solution to this problem in narrowband systems [1]. However, if the harmonics may fall within the band of interest or intermodulation products are substantial, linear filters will be ineffective. In such cases nonlinear filtering is necessary, however this requires that the system be well-characterised. Techniques exist [2] to identify nonlinear systems, but these rely on knowledge—or even control—of the system input, and are therefore inappropriate in cases where the system cannot be calibrated, or where the nonlinearity varies with time.

This type of measurement is prevalent in the testing of analogue-to-digital converters (ADCs). These involve the injection of a given test signal and the measurement of the response. Some test signals include sinusoids [3], triangular signals [3], and Gaussian noise [4]. While these are generally designed to cover the entire input range of the device, some have used smaller-amplitude signals [5] to characterise in small steps the entire input range of the device.

We consider a similar technique, using wideband Gaussian noise superimposed upon the signal of interest to develop a local estimate of the distorting function and so compensate for the system response without the introduction of feedback. However, instead of applying an external test signal, thereby requiring that the system be taken offline, we are able to use the noise of the system input stage, normally considered undesirable, to measure the nonlinearity directly.

We have experimentally demonstrated [6] this technique, however the method used was computationally intensive. We present an improved method that is suitable for real-time implementation in an embedded system.

Other techniques have been considered for online characterisation of digitising systems, however they have been limited in scope. Rahkonen and Kangas [7] describe a technique to compensate for single-bin errors by adjusting bin widths at certain points—such as most-significant-bit transitions—in order to preserve the continuity of the histogram of signal levels. However, this technique is useful only for nonlinearities that are restricted to a few code bins and cannot be used to compensate for those occurring across the entire input range.

Figueiredo, et al. [8] proposed the use of internal noise in pipelined ADCs to produce a uniformly-distributed test signal for the purpose of histogramming. However, unlike our technique, this cannot be performed online, and is restricted to the compensation of pipelined ADCs—it is not suitable for other architectures, nor can it capture nonlinearity that is introduced by other parts of the system.

II. Signal model

We begin as in [6] by considering the simple model shown in Figure 1. Denoting a band-limited signal $x(t)$, a stationary Gaussian noise process $w(t)$ is added, forming an input signal

$$z(t) = x(t) + w(t), \tag{1}$$

and so an output signal

$$y(t) = f(z(t)) = f\left(x(t) + w(t)\right). \tag{2}$$

We also make the assumption that the function $f(z)$ is differentiable over the range of input $z(t)$, and that this derivative $f'(z)$ is everywhere nonzero. The first condition implies that there exists some linearisation about each point, while the second that $f(z)$ is strictly monotonic and so invertible.

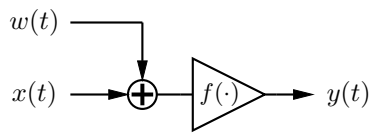

Fig. 1. The combination of a signal $x(t)$ and noise $w(t)$ is amplified by a non-ideal amplifier to produce a distorted signal $y(t)$. We assume that all noise can be reduced to a single stationary additive Gaussian source at the amplifier input.

U.S. Government work not protected by U.S. copyright

III. Online tracking

We base our system on [5], using relatively small fluctuations superimposed on a slowly-varying signal to provide local estimates of the system behaviour. We consider here stationary Gaussian noise due to its natural availability at the amplifier input.

A signal that varies only slowly can be separated from the noise, to a great extent, by low-pass filtering. Conversely, a high-pass filter will produce a signal composed almost entirely of noise. It is the latter signal that is used to characterise the system. If we presume the system to be approximately linear over the range of the noise signal, then the standard deviation $\sigma_o(t)$ of the noise at the output is related to that σ_i at the input by

$$\sigma_o(t) = |f'(x(t))|\sigma_i. \tag{3}$$

Assuming without loss of generality that $f'(x(t)) > 0$,

$$f'(x(t)) = \frac{\sigma_o(t)}{\sigma_i} \tag{4}$$

and so

$$(f^{-1})'(f(x(t))) = \frac{\sigma_i}{\sigma_{o(t)}}. \tag{5}$$

Integrating this, we find the input to be

$$x(t) = x(t_0) + \int_{t_0}^{t} \frac{\sigma_i}{\sigma_o(\tau)} \frac{df(x(\tau))}{d\tau}\, d\tau, \tag{6}$$

where τ is a dummy variable representing the time of the concurrent measurements $f(x(\tau))$ and $\sigma_o(\tau)$.

We might integrate this directly with respect to τ, finding

$$x(t_n) - x(t_0) \approx \sigma_i \sum_{k=1}^{n} \frac{f(x(t_k)) - f(x(t_{k-1}))}{\sigma_o(t_k)}, \tag{7}$$

however errors in the estimated $\hat{\sigma}_o(\tau)$ will accumulate, causing drift.

We know from Eqn. 4 that $\sigma_o(\tau)$ is dependent upon τ only indirectly; in fact, we may write Eqn. 6 in terms of a time-invariant output noise $\bar{\sigma}_o(f(x(\tau)))$:

$$x(t) = x(t_0) + \int_{f(x(t_0))}^{f(x(t))} \frac{\sigma_i}{\bar{\sigma}_o(f(x(\tau)))}\, df(x(\tau)), \tag{8}$$

and integrate numerically to find

$$x(t_n) - x(t_0) \propto \sum_{\substack{k \\ f(x(t_k)) < f(x(t_n))}} \frac{\Delta_k}{\bar{\sigma}_o(f(x(t_k)))}, \tag{9}$$

where Δ_k is equal to $f(x(t_i)) - f(x(t_k))$, the difference between $f(x(t_k))$ and the next largest measurement of $f(x(\cdot))$.

Critically, as $t \to \infty$, the Δ_k will fall linearly with t, reducing the variance of Eqn. 9 at a rate $\mathcal{O}(t^{-1})$ as further samples are processed. Conversely, in Eqn. 7 the weights do not diminish with the number of samples and so errors are simply added, causing the variance of the estimate to increase at a rate $\mathcal{O}(t)$.

This asymptotic behaviour comes at a cost, however—whereas Eqn. 7 can be evaluated recursively, Eqn. 9 requires knowledge of all noise estimates up to that point. This is impractical, and we must therefore consider more efficient ways to approximate Eqn. 8.

A. Degradation of noise measuremenst

We take a moment to briefly discuss the effects of other elements of the system such as additional noise sources and filtering.

Perhaps the greatest concern is the effect of bias due to excess noise appearing at the ADC input. In this case, Eqn. 3 must be augmented with an extra term representing the excess noise σ_x^2:

$$\sigma_o(t) = \sqrt{|f'(x(t))|^2\sigma_i^2 + \sigma_x^2}. \tag{10}$$

Therefore, the estimated gain will be

$$\hat{f}'(x(t)) = \sqrt{|f'(x(t))|^2 + \frac{\sigma_x^2}{\sigma_i^2}}, \tag{11}$$

resulting in an overestimated differential gain. This could be ameliorated by subtracting the constant bias term σ_x^2/σ_i^2 from the measured power, however the online estimation of this quantity is beyond the scope of this paper. This term also includes harmonics of the signal being measured, and therefore greater accuracy is achievable in systems with a wider noise bandwidth that extends beyond the measurable distortion products of the signal. Filtering between amplifier stages will exaggerate this effect by reducing σ_i^2, however our analysis within the remainder of this section does not depend upon an assumption of whiteness.

IV. Transfer function approximation

Rather than attempting to directly integrate Eqn. 8 as in Eqn. 9, we instead construct an approximation $\hat{g}(f(x(t)))$ of $1/\bar{\sigma}_o(f(x(t)))$ that is amenable to recursive estimation.

We begin with three criteria for our approximation: first, it should be possible to efficiently compute arbitrary indefinite integrals without resort to numerical integration; second, it should be continuous in order that its integral is everywhere differentiable and so does not contain sharp corners that would produce large amounts of harmonic content; third, it should be able to model a constant function exactly in order that a linear system can be represented. These criteria are satisfied by continuous piecewise linear functions, which we construct as the sum of radial basis functions [9].

We have selected basis functions of the form

$$r(x) = \begin{cases} 1 - |x|/\Delta & \text{if } x \in [-1, +1] \\ 0 & \text{otherwise,} \end{cases} \tag{12}$$

uniformly spaced Δ apart as shown in Figure 2. The number of basis functions that are used and the value of Δ are chosen according to the desired domain of approximation and the level of detail that is to be represented. The basis function widths are chosen to be 2Δ so that exactly two basis functions will cover each point, except at the centres of each basis function $r_k(x)$. The two basis functions will have opposing slopes,

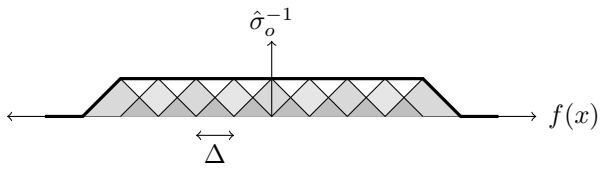

Fig. 2. Basis functions for differential gain approximation, as described in Eqn. 12. Triangular basis functions are chosen so that equally-weighted basis functions will sum to a constant function over the range of interest.

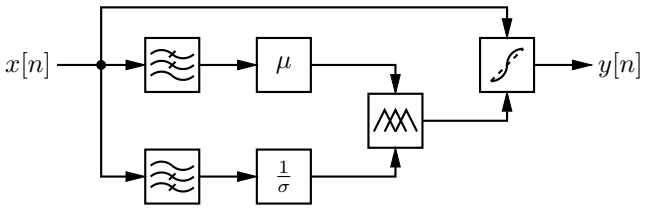

Fig. 3. Adaptive compensator block diagram. Filters are used to separate signal from noise, and the mean and inverse standard deviation respectively are calculated from small blocks of samples. These are used to update the basis coefficients of the differential gain approximation, which is periodically integrated to update the distortion compensation function.

allowing a constant function to be trivially represented by equally-weighting adjacent basis functions.

The scaling coefficients c_n of each basis function are computed as a weighted average of the measured inverse-standard-deviations,

$$c_k[n] = \frac{\sum_{i=0}^{n} r_k(f(x(t_i)))\ \hat{\sigma}_o^{-1}(t_i)}{\sum_{i=0}^{n} r_k(f(x(t_i)))}, \tag{13}$$

with the weights proportional to the unweighted basis function. In order to accommodate variation over time of the distorting transformation f, we allow the weights to decay with time, resulting in the following estimation scheme:

$$a_k \longleftarrow \gamma a_k + (1-\gamma) r_k(f(x(t_i)))\hat{\sigma}_o^{-1}(t_i) \tag{14}$$
$$w_k \longleftarrow \gamma w_k + (1-\gamma) r_k(f(x(t_i))), \tag{15}$$

with the coefficients c_n computed as

$$c_k = a_k / w_k. \tag{16}$$

In practice we update only the coefficients of the two basis functions containing the current measurement within their supports.

Having constructed an approximation $\hat{g}(f(x(t)))$ of $1/\sigma_o(f(x(\tau)))$, we must now evaluate the integral from Eqn. 9. The form of $r(x)$ allows this to be performed analytically:

$$\hat{x}(t) = \int_{-\infty}^{f(x(t))} \hat{g}(u)\ du \tag{17}$$
$$= \int_{-\infty}^{f(x(t))} \sum_{k=-\infty}^{\infty} c_k r(u - k\Delta)\ du. \tag{18}$$

Letting $n < f(x(t))/\Delta < n+1$, we use the fact that $\int_{-\infty}^{\infty} r(u)\ du = \Delta$ to simplify this to

$$= \sum_{k=-\infty}^{n-1} c_k \Delta \tag{19}$$
$$+ \int_{-\infty}^{f(x(t))} c_n r(u - n\Delta) + c_{n+1} r(u - (n+1)\Delta)\ du. \tag{20}$$

Noting that in this region the two terms are linear functions with slopes $-c_n/\Delta$ and c_{n+1}/Δ respectively, we make the substitution $v = u - n\Delta$ to produce

$$= \sum_{k=-\infty}^{n-1} c_k \Delta + \frac{1}{2} c_n \Delta \tag{21}$$
$$+ \int_{0}^{f(x(t))-n\Delta} \Delta(c_{n+1} - c_n)u + c_n\ du \tag{22}$$
$$= \sum_{k=-\infty}^{n-1} c_k \Delta + \frac{1}{2} \Delta c_n \tag{23}$$
$$+ (f(x(t)) - n\Delta)\, c_n \tag{24}$$
$$+ (f(x(t)) - n\Delta)^2\, \frac{c_{n+1} - c_n}{2\Delta}. \tag{25}$$

This piecewise quadratic function may be evaluated far more efficiently than Eqn. 9, paving the way for real-time implementation.

V. Implementation

We have implemented the technique described above on an STM32F407 microcontroller; the demonstration system is shown in Figure 4. Source code [10] is available.

The system operates at a sampling rate of 1.55 MHz, using the on-board ADCs and DACs of the microcontroller. A block size of four samples is used, with a block computed and processed at 128-sample intervals. The computed $\hat{g}(\cdot)$ has 256 basis functions and is integrated every 1024 blocks to produce the corresponding piecewise polynomials.

Samples from the ADC are low-pass filtered to produce an estimate of the signal; this is subtracted from the original sample to produce an estimate of the signal's noise component. The compensating transformation is applied to the original (pre-filter) samples, and the results scaled and offset to match the DAC output range.

A. Triangular waves

In an attempt to describe the function of the device qualitatively, we have applied a distorted triangular wave to the device, with results shown in Figure 5. The amplifier distorts the wave to the point that one can no longer recognise its true form, however after compensation the wave is almost indistinguishable from its ideal form.

The use of triangular waves allows simple histogram measurements [3] to determine integral and differential nonlinearity (INL and DNL respectively). We measured histograms using an HP35665A Dynamic Signal Analyser, producing the

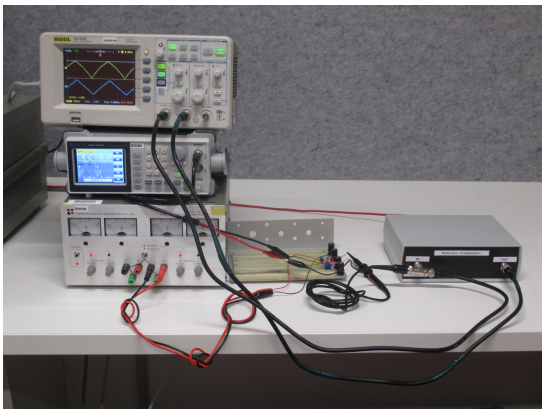

Fig. 4. The distortion compensator unit in operation. A signal generator (left) produces a ramp signal, which is distorted by the transistor amplifier (centre), and processed by the compensator (right). Examples of the measured waveforms are provided in Figures 5 and 8.

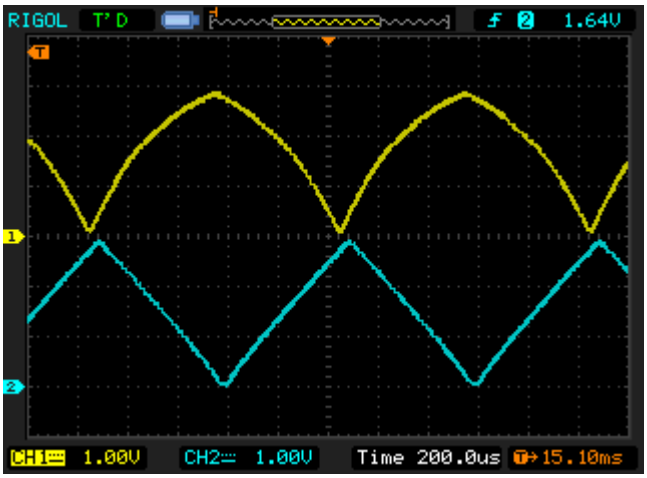

Fig. 5. The compensator applied to a distorted triangle wave. The top signal is produced by applying a 50 mV, 1 kHz triangle wave to the base of a bipolar transistor configured as a common-emitter amplifier with rails of 0 V and 3 V. This is provided as input to the compensator, which produces the far less distorted signal underneath.

results in Figure 6. The improvement in differential nonlinearity is of particular note, remaining relatively flat over the entire range in comparison with the distorted signal with its enormous variation.

B. Total harmonic distortion measurements

Total harmonic distortion (THD) provides an alternative measure of distortion. We apply a sinusoidal signal to the distorting amplifier, and simultaneously measure the spectrum of the output before and after compensation. The THD of a signal with respect to the fundamental frequency f_0 is defined as

$$\mathrm{THD} = \sqrt{\frac{\sum_{n=1}^{\infty} |X(nf_0)|^2}{|X(f_0)|^2}}, \tag{26}$$

where $X(f)$ is the Fourier transform of the distorted signal.

We measure the first five harmonics and compute the THD before and after compensation, shown in Figure 7.

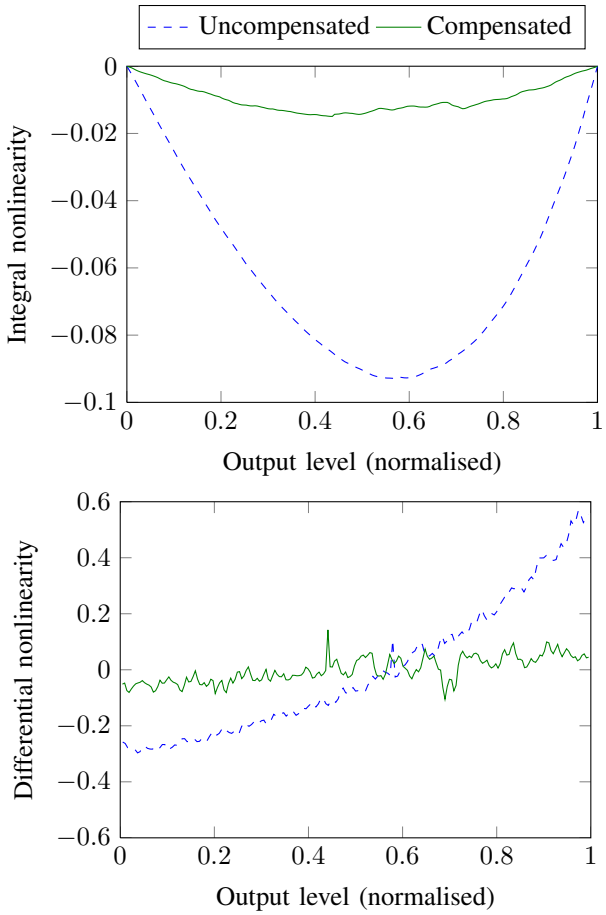

Fig. 6. Measured integral and differential nonlinearity of the amplifier before and after compensation. By both measures, the compensation process has substantially improved the linearity of the amplifier. Linearity is calculated across the central 90% of the measurement range in order to remove measurement artifacts.

We see that the technique described above provides a substantial improvement in performance, especially at low signal levels where a reduction of 17 dB has been achieved. However, an improvement of more than 10 dB is possible even in the case of large input signals such as shown in Figure 8.

VI. Conclusion

We have demonstrated a practical technique for adaptive compensation of nonlinear distortion. The use of radial basis functions allows the post-distortion technique of [6] to be implemented using a compact device model that can be evaluated quickly and is suitable for implementation within an embedded system. We have demonstrated this technique experimentally on a microcontroller, showing the ability to reduce the total harmonic distortion of a single-transistor amplifier by approximately 15 dB using real-time postprocessing.

References

[1] C. Coleman, *An Introduction to Radio Frequency Engineering*. Cambridge University Press, 2004.

[2] L. Ljung, *System Identification: Theory for the User*. Prentice Hall, 1987.

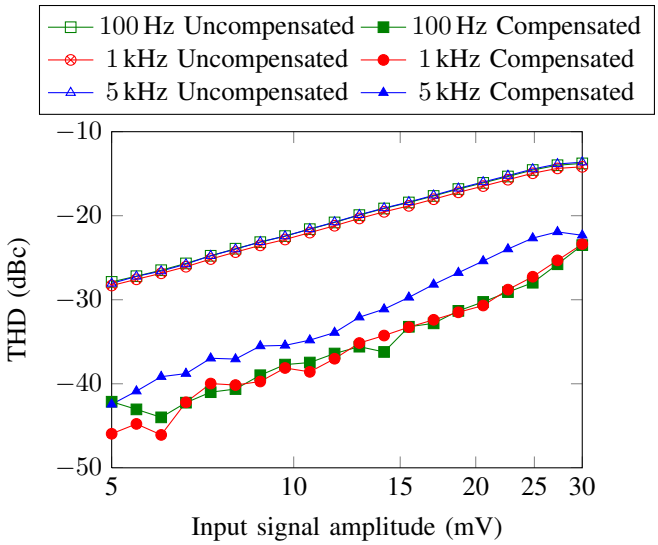

Fig. 7. Measured total harmonic distortion (THD) of a common-emitter amplifier as a function of input voltage at 100 Hz, 1 kHz and 5 kHz, before and after compensation. At low signal levels (below around 10 mV input) an improvement of about 15 dB is achieved at 1 kHz and below.

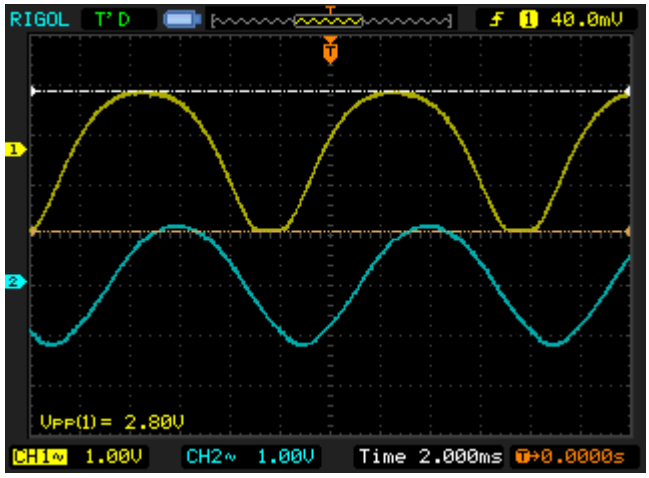

Fig. 8. The compensator applied to a distorted sinusoid. Note that detail is extracted even from the base of the signal where the amplifier is heavily saturated.

[3] "IEEE standard for digitizing waveform recorders," *IEEE Std 1057-2007 (Revision of IEEE 1057-1994)*, pp. c1–142, 2008.

[4] R. Martins and A. da Cruz Serra, "Automated ADC characterization using the histogram test stimulated by Gaussian noise," *IEEE Transactions on Instrumentation and Measurement*, vol. 48, no. 2, pp. 471–474, 1999.

[5] F. Alegria, P. Arpaia, A. da Cruz Serra, and P. Daponte, "ADC histogram test by triangular small-waves," in *Proc. 18th IEEE Instrumentation and Measurement Technology Conference*, vol. 3, Budapest, Hungary, 2001, pp. 1690–1695.

[6] L. J. Gunn, A. Allison, and D. Abbott, "Identification of static distortion by noise measurement," *Electronics Letters*, vol. 49, no. 21, pp. 1321–1323, 2013.

[7] T. Rahkonen and M. Kangas, "Histogram based background correction of ADC," in *Proc. Norchip Conference*, Oslo, Norway, 2004, pp. 95–98.

[8] M. Figueiredo, N. Paulino, G. Evans, and J. Goes, "New simple digital self-calibration technique for pipeline ADCs using the internal thermal noise," in *Proc. IEEE Int. Symp. on Circuits and Systems*, May Seattle, USA, 2008, pp. 232–235.

[9] M. D. Buhmann, "Radial basis functions," *Acta Numerica*, vol. 9, pp. 1–38, 2000.

[10] L. J. Gunn, A. Allison, and D. Abbott. Stochastic instrumentation tools. [Online]. Available: https://github.com/LachlanGunn/stochastic-instrumentation-tools/

SiPS 2014

2014 IEEE Workshop on Signal Processing Systems

Queen's University Belfast
UK

October 20th - 22nd 2014

Proceedings of the 2014 IEEE Workshop on Signal Processing Systems

IEEE Cat. Num: CFP14SIG-USB
ISBN: 978-14799-6578-8